applied sciences

MDPI

Article

Hybrid Huff-n-Puff Process for Enhanced Oil Recovery: Integration of Surfactant Flooding with CO_2 Oil Swelling

Abhishek Ratanpara [1], Joshua Donjuan [1], Camron Smith [1], Marcellin Procak [2], Ibrahima Aboubakar [2], Philippe Mandin [2], Riyadh I. Al-Raoush [3], Rosalinda Inguanta [4] and Myeongsub Kim [1,*]

[1] Department of Ocean and Mechanical Engineering, Florida Atlantic University, Boca Raton, FL 33431, USA; aratanpara2020@fau.edu (A.R.); camronsmith2021@fau.edu (C.S.)
[2] IRDL UMR CNRS 6027, Université de Bretagne Sud (UBS), 56100 Lorient, France; aboubakaribrahim371@gmail.com (I.A.); philippe.mandin@univ-ubs.fr (P.M.)
[3] Department of Civil and Environmental Engineering, Qatar University, Doha P.O. Box 2713, Qatar
[4] Department of Engineering, Università degli Studi di Palermo, Viale delle Scienze, 90128 Palermo, Italy; rosalinda.inguanta@unipa.it
* Correspondence: kimm@fau.edu

Abstract: With increasing energy demands and depleting oil accessibility in reservoirs, the investigation of more effective enhanced oil recovery (EOR) methods for deep and tight reservoirs is imminent. This study investigates a novel hybrid EOR method, a synergistic approach of nonionic surfactant flooding with intermediate CO_2-based oil swelling. This study is focused on the efficiency of surfactant flooding and low-pressure oil swelling in oil recovery. We conducted a fluorescence-based microscopic analysis in a microchannel to explore the effect of sodium dodecyl sulfate (SDS) surfactant on CO_2 diffusion in Texas crude oil. Based on the change in emission intensity of oil, the results revealed that SDS enhanced CO_2 diffusion at low pressure in oil, primarily due to SDS aggregation and reduced interfacial tension at the CO_2 gas–oil interface. To validate the feasibility of our proposed EOR method, we adopted a 'reservoir-on-a-chip' approach, incorporating flooding tests in a polymethylmethacrylate (PMMA)-based micromodel. We estimated the cumulative oil recovery by comparing the results of two-stage surfactant flooding with intermediate CO_2 swelling at different pressures. This novel hybrid approach test consisted of a three-stage sequence: an initial flooding stage, followed by intermediate CO_2 swelling, and a second flooding stage. The results revealed an increase in cumulative oil recovery by nearly 10% upon a 2% (w/v) solution of SDS and water flooding compared to just water flooding. The results showed the visual phenomenon of oil imbibition during the surfactant flooding process. This innovative approach holds immense potential for future EOR processes, characterized by its unique combination of surfactant flooding and CO_2 swelling, yielding higher oil recovery.

Keywords: huff-n-puff; EOR; chemical EOR; carbon capture and storage; surfactant flooding; reservoir-on-a-chip

Citation: Ratanpara, A.; Donjuan, J.; Smith, C.; Procak, M.; Aboubakar, I.; Mandin, P.; Al-Raoush, R.I.; Inguanta, R.; Kim, M. Hybrid Huff-n-Puff Process for Enhanced Oil Recovery: Integration of Surfactant Flooding with CO_2 Oil Swelling. *Appl. Sci.* **2024**, *14*, 12078. https://doi.org/10.3390/app142412078

Academic Editor: Tiago Miranda

Received: 25 October 2024
Revised: 18 December 2024
Accepted: 20 December 2024
Published: 23 December 2024

1. Introduction

Energy demands continuously grow due to technological advancements, leading to concerns about meeting these increased needs. According to the Institute for Energy Research, energy consumption will increase by roughly 50% in 2050 [1]. Fossil fuels have always been the primary energy source for humankind, and this trend will continue for the foreseeable future to meet the energy demand. Despite significant attempts to shift the energy source to other nonconventional and environmentally friendly sources, fossil fuels have stayed the primary source of energy supply. Among various resources, crude oil contributed 46.2% of total energy demand in 1973 and still accounts for almost 31% as of 2019, proving to be the highest among all the energy sources [2]. These data show that crude oil is an indispensable energy reserve to mitigate the energy crisis until a prominent

environmentally friendly option is available. Unfortunately, crude oil is continuously depleting, as its reserve is finite [3]. Therefore, oil extraction must be performed as efficiently as possible to maintain the proportional oil supply. Fortunately, numerous enhanced oil recovery (EOR) methods have been implemented to recover as much oil as possible from depleted reservoirs.

The conventional oil extraction process has been mainly classified into three stages. The first stage, or primary stage, is where oil is naturally extracted by five driving forces: dissolved gas-driven, water-driven, gravity drainage-driven, gas cap-driven, and combination-driven [4]. Even with the aid of additional pumping systems to pump the oil out of the production well, the first stage of oil recovery produces a small percentage of the original oil in place (OOIP). It is then followed by the second stage of oil recovery, where external fluids like water and gas are flooded through strategically located wells around the production well to recover more oil through a volumetric sweep by maintaining the positive pressure in the reservoir. Both first- and second-stage oil recovery produces around 33% of the OOIP [5]. Even with the implementation of two stages, approximately 65% of OOIP remains in the reservoir because the oil is trapped within small pores of the heterogeneous reservoir structure with higher capillary forces and viscosity [6].

The tertiary recovery stage, or EOR, is implemented to extract the remaining oil using various methods like thermal, chemical injections, and gas injections [7]. These methods alter the reservoir surface and oil properties, including wettability, interfacial tension (IFT), viscosity, and capillary pressure, potentially leading to increased oil recovery. Different EOR methods are implemented based on the reservoir conditions. Thermal methods like stem injection, electrical heating, and various energy input techniques are used to increase the reservoir temperature, reduce oil viscosity, and increase oil mobility [8]. In chemical methods, various surfactants, nanoparticles, or polymers are used to alter the wettability of the reservoir surface to make it more water-wet by reducing the IFT of oil and flooding fluid [9,10]. In gas EOR, air, carbon dioxide (CO_2), nitrogen (N_2), and water, alternating gas injections are used to reduce oil viscosity. This is achieved through the expansion of oil volume by gas dissolution and the miscibility between oil and gas [11]. Among all these EOR methods, thermal methods account for 67% of all the global EOR projects due to their comparatively high performance [8]. However, thermal methods cannot be applied effectively in deep reservoirs or thin pay zone reservoirs, which contain comparatively narrow hydrocarbon layers, primarily due to significant heat losses in these environments [12]. Moreover, thermal techniques are energy-intensive and have higher operational costs, limiting their feasibility in regions with challenging geological conditions. As exploration ventures deeper into the earth's crust, the increasing reservoir depth and high pressures make thermal methods less efficient and economically unviable. Chemical EOR methods, while promising, often face challenges such as surfactant adsorption onto the reservoir rock, which reduces the active concentration of the chemicals and limits their effectiveness. In addition, gas injection methods like CO_2 flooding, though widely studied, suffer from low sweep efficiency and gas channeling in heterogeneous reservoirs, leading to incomplete oil displacement. Particularly, CO_2-based EOR methods have emerged as a focal point of research due to their dual benefits: enhancing oil recovery and simultaneously providing a means for carbon storage, thus contributing to climate change mitigation. Despite these advances, there remains a need for innovative approaches that improve CO_2 utilization efficiency and address surfactant loss, interfacial tension reduction, and oil mobility, particularly in low-pressure reservoirs.

To overcome these limitations, hybrid methods that combine chemical and gas-based EOR strategies have drawn significant attention [13,14]. Particularly, CO_2-based EOR methods have emerged as a focal point of research due to their dual benefits: enhancing oil recovery and simultaneously providing a means for carbon storage, thus contributing to climate change mitigation. Despite these advances, there remains a need for innovative approaches that improve CO_2 utilization efficiency and address surfactant loss, interfacial tension reduction, and oil mobility, particularly in low-pressure reservoirs. Oilfield devel-

opment and CO_2 flooding have an impact on the development of the oil industry in terms of EOR [15,16].

Many approaches related to CO_2 injection-based EOR are available, including continuous CO_2 injection, water alternate CO_2 injection, and a CO_2-based huff-n-puff method. The huff-n-puff method is considered the most effective among all the CO_2-based EOR methods [12]. In this method, high-pressure CO_2 is injected into the oil reservoir, and oil is mobilized. This is followed by a soaking period, during which the reservoir is sealed while CO_2 is dissolved into the oil [17,18]. During this period, the oil swells and becomes less viscous due to CO_2 dissolution. In the final stage, the well is opened, and the swollen oil is recovered due to the driving force generated by injected CO_2 pressure [19]. This method could be further improved by integrating chemical flooding. Recently, the potential of the nonionic polyether surfactant-assisted huff-n-puff method was tested in the core-based flooding experimental research [20]. It was found that additional surfactant flooding improved 14–19% of oil recovery compared to only the huff-n-puff method [20]. These promising results led us to propose a novel method of using an anionic surfactant flooding with intermittent CO_2 swelling.

The primary hypothesis of this study is that the strategic implementation of surfactant flooding before and after a CO_2-induced oil swelling stage can significantly enhance oil recovery. Initially, surfactant flooding recovers more oil by using the wettability alteration mechanism, where the surfactant is absorbed by the immobile oil and changes the wettability of the reservoir rock to be more water-wet [21]. This absorption process not only aids in immediate oil recovery but also prepares the oil for subsequent stages. Following this, oil swelling is induced by CO_2 injection. The absorbed surfactant during the initial flooding helps to enhance the oil swelling process by improving the CO_2 solubility in oil, resulting in greater oil volume expansion and better mobilization within the reservoir. Finally, a second stage of surfactant flooding is performed to mobilize the swelled oil, which is easier to extract due to its reduced viscosity. Additionally, this second flooding gets access to the small pores that were not accessible during the initial flooding. By combining these stages, the study aims to maximize oil recovery through the synergistic effects of surfactant absorption, wettability alteration, CO_2 dissolution, and oil mobilization. This sequential approach not only enhances oil swelling but also ensures that more oil is tapped from previously inaccessible areas of the reservoir, leveraging the surfactant absorbed during the initial flooding to facilitate greater CO_2-induced swelling.

To investigate this hypothesis, we have chosen to use a microfluidic approach. Previously published literature has validated microfluidic approaches in EOR studies, such as 'lab-on-a-chip' and 'reservoir-on-a-chip', due to their excellent experimental framework with precise reproduction and economic feasibility [22–24]. In this study, we have conducted two types of experiments: a fluorescence-based microscopic experiment and a microfluidic reservoir-based flooding experiment. A fluorescence-based microscopic experiment was conducted to investigate the effect of SDS surfactant on CO_2 dissolution in oil, providing crucial insights into the chemical reactions involved. A micro reservoir flooding experiment was performed to investigate the improvement in oil recovery using the proposed method, demonstrating its practical applications. All the experiments were performed at low CO_2 pressure, as the experimental goal is solely to demonstrate the potential of the proposed hybrid huff-n-puff in EOR.

2. Materials and Methods

2.1. Materials

CO_2 (Research 5.0 Grade–99.999% purity) was obtained by Airgas, Inc. (Radnor, PA, USA). Sodium dodecyl sulfate (SDS, >99% purity) was purchased from Sigma Aldrich (St. Louis, MO, USA). Polymethylmethacrylate (PMMA) clear sheets were purchased from McMaster-Carr (Elmhurst, IL, USA). Texas crude oil (density 796 kg/m^3 and viscosity 27.26 cP) was used for the experiments.

2.2. Experimental Method

2.2.1. Fluorescence-Based Oil Swelling

To implement an accurate quantification of time-dependent oil swelling by SDS and CO_2 gas, we prepared a microfluidic platform consisting of a PMMA channel (1.5 mm (W) × 5 cm (L) × 1 mm (H)), inlet and outlet ports connected to the injection solutions and a Petri dish, respectively. The thickness of the microchannel was chosen to be 1000 µm to guarantee one-dimensional (1D) diffusion of CO_2 gas into oil. It should be noted that PMMA has excellent transmission of visible light (>92%), suitable for direct optical microscopy. PMMA sheets were cut using a laser cutter (Universal Laser Systems, Inc., VLS 2.30, Scottsdale, AZ, USA) with a unique AutoCAD design. As shown in Figure 1, the PMMA sheet containing the microchannel was stacked with two other PMMA sheets, top and bottom. The top sheet was cut to create two holes for the inlet and outlet ports, while the bottom sheet was kept plain. These three sheets were thermally bonded in a sandwich-style arrangement to create a trapped microchannel in the middle. For thermal bonding, a solution with a 7:3 ratio of isopropyl alcohol (IPA) and ethanol was used between the sheets, and then the PMMA assembly was placed in the oven for 30 min at 50 °C. The 50 °C was used to keep the channel's shape intact [25]. A special nano port fitting (IDEX Health & Science, N-333, Manhattan, NY, USA) was clamped with two additional PMMA sheets (3.175 mm thick) and four screws to ensure effective injection of CO_2 without leakage. Approximately 90 µL of oil was injected into the microchannel using the syringe pump, and the inlet was carefully closed. A pressure controller was used to maintain the CO_2 gas at a constant pressure on the other end of the channel. The microchannel was placed under the UV light source (Figure 1). Crude oil naturally exhibits autofluorescence due to the presence of polycyclic aromatic hydrocarbon (PAH) compounds under UV light, which changes its emission intensity because of its swelling upon CO_2 dissolution [26,27]. Figure 1b shows an example of experimental images of oil's emission change in the microchannel over time under constant CO_2 pressure.

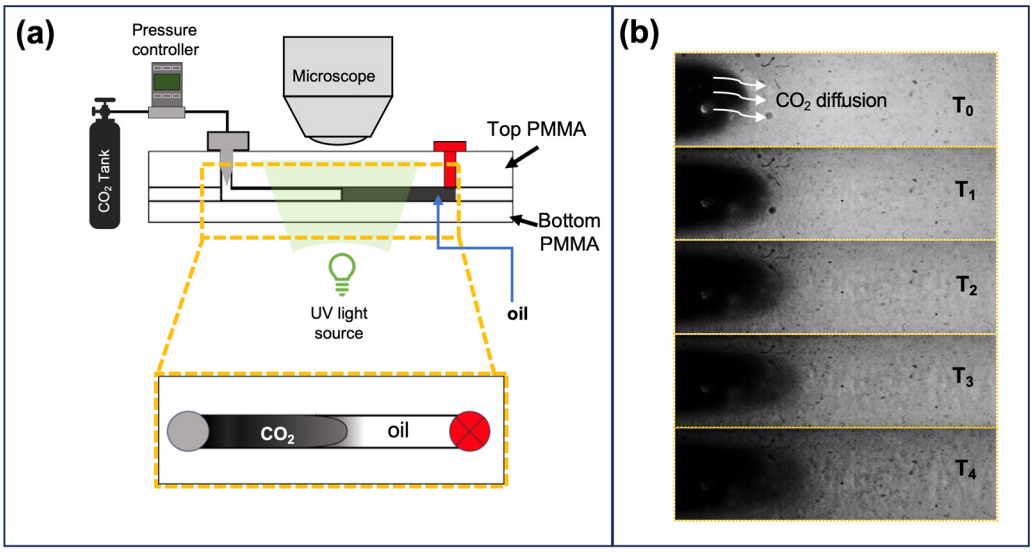

Figure 1. (**a**) Illustrative image of experimental set up. (**b**) Actual experimental results, showing the change in emission intensity of oil over time due to CO_2 dissolution.

2.2.2. Flooding Experiments in Micromodels

For flooding experiments, we employed a 'reservoir-on-a-chip' approach in micromodels. PMMA-based micro reservoirs containing random pore structures were engraved over the 50 mm × 25 mm engraved area with a laser cutter. The porous network was generated by MATLAB random network generation code and modeled in AutoCAD 2022. The engraved surface was analyzed by a 3-D profilometer (Keyence, VR-6100, Itasca, IL,

USA), as shown in Figure 2. The analyzed images show that the average pore depth of the micro reservoir is 1 mm, with minimum and maximum depths of 0.25 mm and 1.997 mm, respectively. The pore volume of the entire reservoir was estimated to be 200 µL.

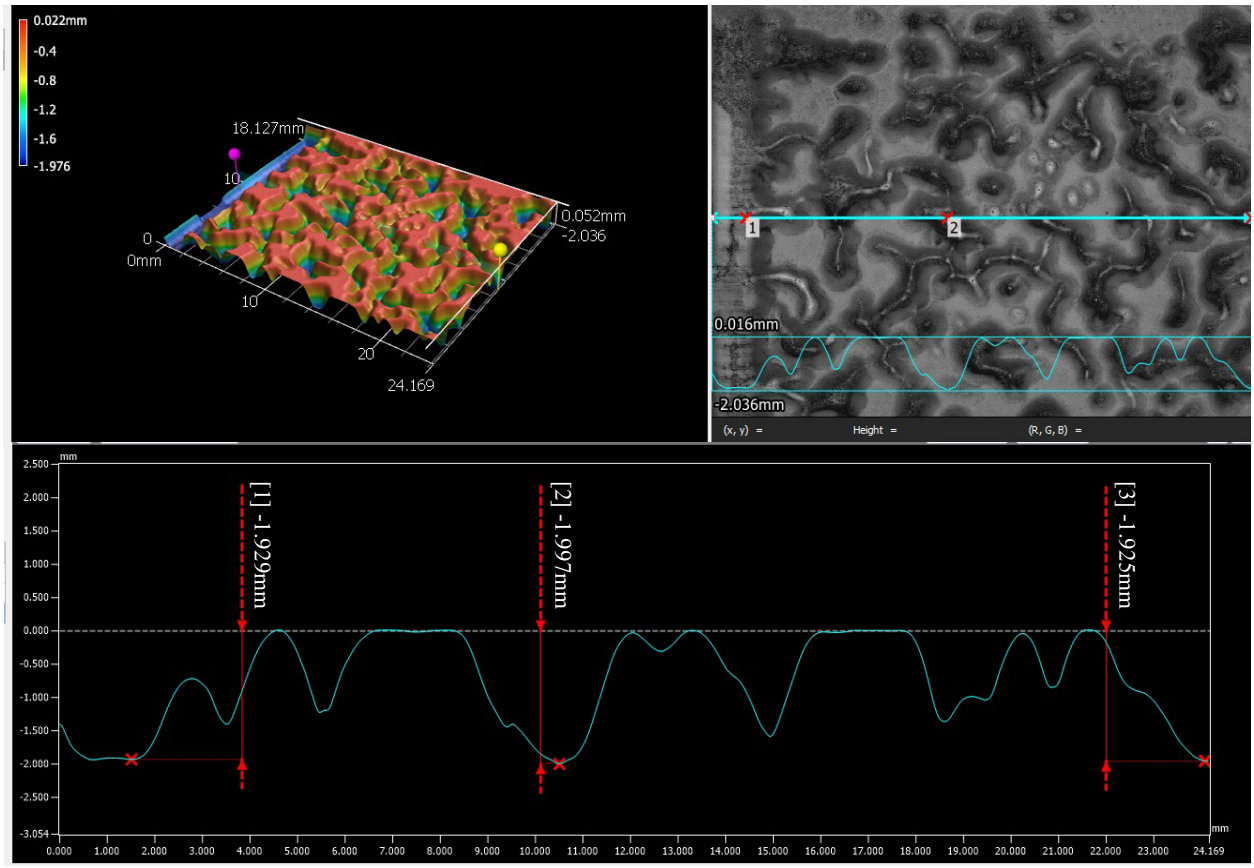

Figure 2. The 3-D profile scan of the reservoir surface by a 3D profilometer (Top left). The linear measurement of the depth analysis for different pores (top right and bottom).

The engraved PMMA surface was thermally bonded with another PMMA sheet with the two inlet and outlet holes (Figure 3b). Thermal bonding and nano port fittings were performed in the same manner as described in Section 2.2.1. The crude oil was filled into the vacuumed porous media to minimize air entrapment during oil injection. After the oil was filled into the porous media, the flooding solutions were injected at 20 µL/min for 30 min as first-stage flooding. The 30 min duration was decided based on the experimental trials, where further oil recovery is negligible. Following the flooding, CO_2 gas was injected into the reservoir, and the outlet was closed for 6 h to simulate the soaking stage of the conventional huff-n-puff process. The 6 h time duration range was selected with reference to previously published articles [28]. Lastly, the reservoir was flooded again with the same flow rate for the same duration as the first flooding. This experiment was conducted with deionized (DI) water flooding and 2% (w/v) SDS-based DI water (SDS-DI water) solution flooding, respectively, at 5, 10 and 15 psig CO_2 gas pressures. As shown in Figure 3a, the experiment was recorded with a Logitech camera at 30 frames per second. The oil swelling stage was recorded as a time-lapse where there is a 30 s interval between each frame to conserve the computation time. The recorded data were analyzed using MATLAB R2022b to quantify the oil produced in each test. Each test was conducted using a new microchannel Each test was conducted using a new microchannel as the PMMA fabrication is inexpensive and to avoid any potential error related to cleaning and washing.

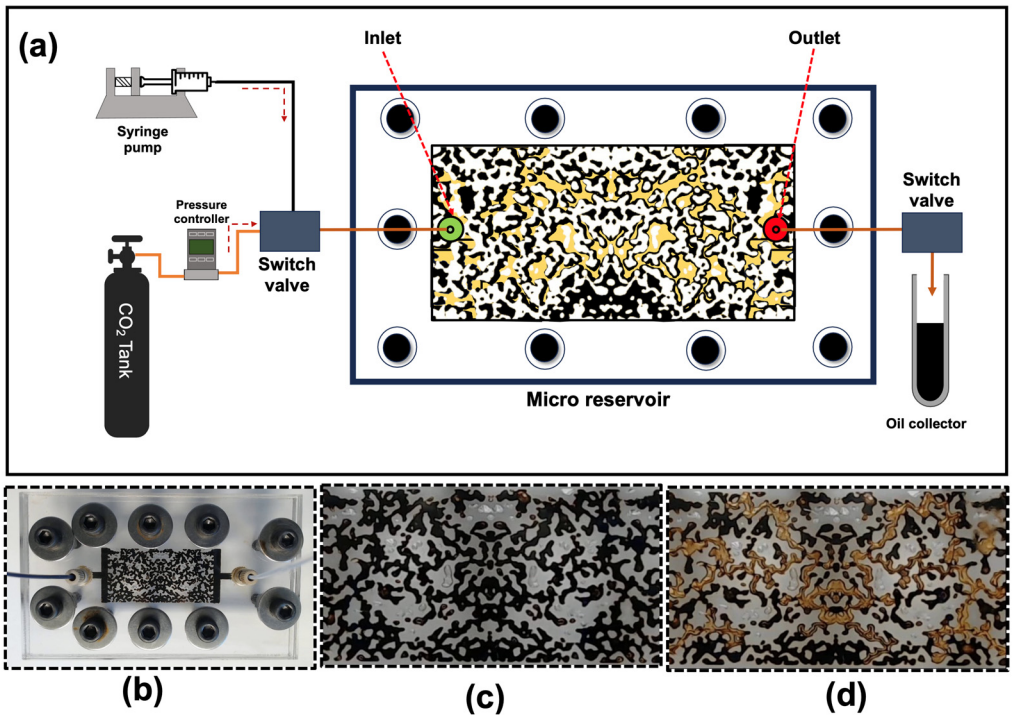

Figure 3. (**a**) Illustrative experimental set up for flooding experiment in a micromodel. (**b**) Actual image of the micro reservoir chip. (**c**) Optical microscopy image of the reservoir filled with oil. (**d**) Optical microscopy image of the reservoir after SDS-DI water flooding.

3. Results and Discussion

3.1. SDS on CO_2-Induced Oil Swelling

CO_2 dissolution in oil is a well-established and published topic as it creates oil swelling and reduces the oil viscosity, subsequently making the oil more mobile [29]. This process is slow and requires high CO_2 pressure to see the measurable change of oil properties on a large scale. Many experiments have been conducted on a microscale to observe the property change and oil swelling at low pressures [30,31]. In the microfluidic approach, CO_2 dissolution and its rate are usually estimated based on image analysis. Therefore, we conducted a fluorescence-based microscopic experiment to investigate the effect of SDS on CO_2 dissolution in oil. Using fluorescence microscopy, we observed the time-dependent intensity change of oil at the CO_2–oil interface in a closed-ended microchannel under constant CO_2 pressure. The changes in fluorescence intensity of the oil according to its concentration provide a visual representation of the CO_2 dissolution process, enabling a comparative study under different conditions without the need for dissolution units [29]. Our study is intended to compare the effect of SDS on CO_2 diffusion in oil, i.e., oil swelling, instead of measuring the absolute CO_2 diffusion and dissolution rate in the oil. We analyzed these effects using pure crude oil with 2% (w/v) SDS.

Figure 4 presents the changes in normalized fluorescence intensity along a microchannel filled with pure crude oil and 2% (w/v) SDS mixed oil at CO_2 pressures of 5 and 10 psig. Each plot includes data collected at 0, 180, and 360 min after oil was pressurized under identical flow conditions. Initially, the fluorescence intensity is zero, indicating no oil presence at that point. The abrupt intensity changes depict the CO_2 –oil interface, which was consistently positioned at the start of CO_2 injection. As CO_2 diffuses into the oil, the fluorescence intensity decreases from the interface along the channel over time (0, 180, 360 min) due to oil swelling. Figure 4a,b show the change in normalized oil intensity in pure oil and SDS mixed oil at 5 psig CO_2 pressure, respectively. It shows that the rate change in intensity is comparatively prominent in SDS mixed oil over time (from 0 min to 180 min and to 360 min). Similarly, the rate change in intensity is more significant at 10 psig CO_2 pressure upon SDS addition. Figure 4d represents the highest intensity change

or, indirectly, the highest CO_2 dissolution in oil among all cases. Overall, the SDS-mixed oil shows higher intensity transitions compared to pure oil, indicating better CO_2 diffusion.

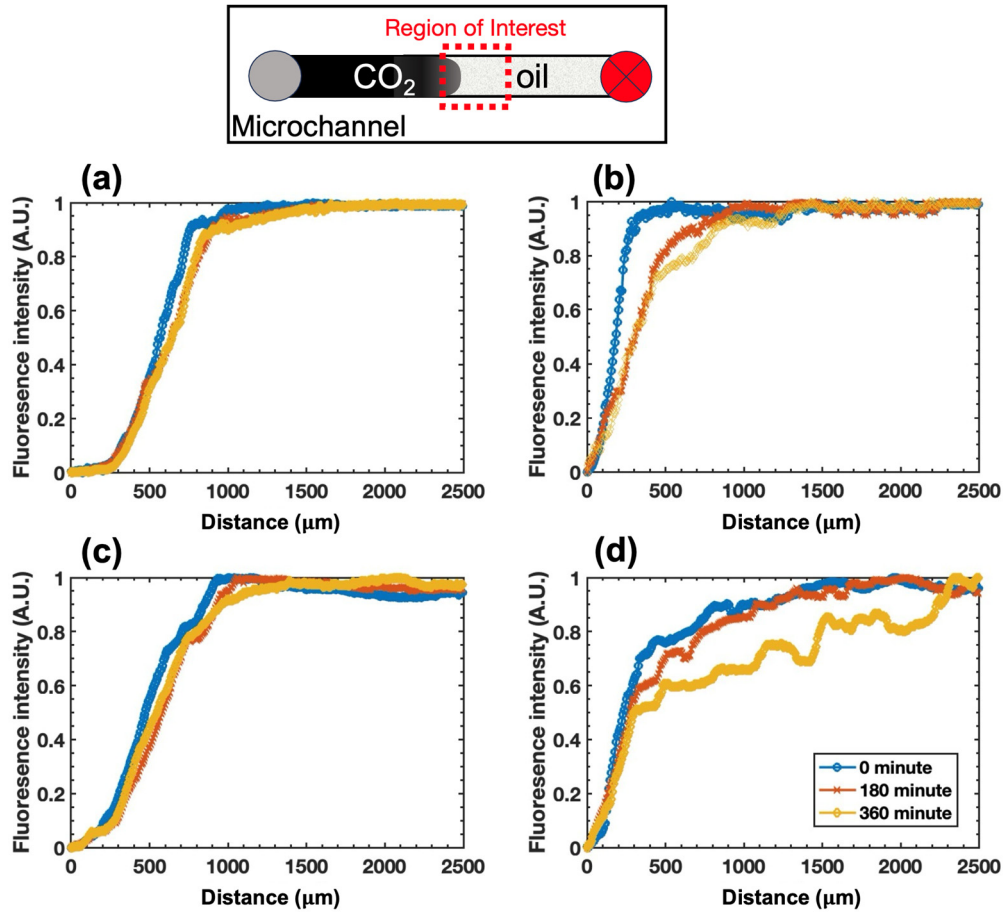

Figure 4. An illustrative image showing the intensity profile location in a microchannel. Fluorescent intensity profiles for pure oil and SDS-mixed oil along the channel at three different time intervals: 0 min, 180 min, and 360 min. (**a**) Pure oil at 5 psig CO_2 pressure. (**b**) 2% (w/v) SDS mixed oil at 5 psig CO_2 pressure. (**c**) Pure oil at 10 psig CO_2 pressure. (**d**) 2% (w/v) SDS mixed oil at 10 psig CO_2 pressure.

To quantify the CO_2 diffusion rate into oil, exponential curve fitting was applied to the normalized intensity values from 0.2 to 1, excluding initial values, to avoid the CO_2-oil interface effect. Figure 5 shows the normalized fluorescent intensity along the microchannel for pure oil and SDS-mixed oil at 180 and 360 min, along with their exponential fits. Although they show some variations in the changes in normalized fluorescence intensity over time, it reaches its saturation, which is 1, at a distance of approximately 2000 or 2500 μm from the oil-CO_2 interface, indicating negligible CO_2 diffusion effect at this location. This behavior can be clearly seen in the asymptotic behavior beyond 0.9 intensity in all cases. A shorter distance for the same intensity change implies a steeper exponential curve, which indicates faster CO_2 diffusion. The distance of the intensity changes allows us to evaluate the relative diffusion rate of CO_2 in oil under different injection pressures and oil surface tension.

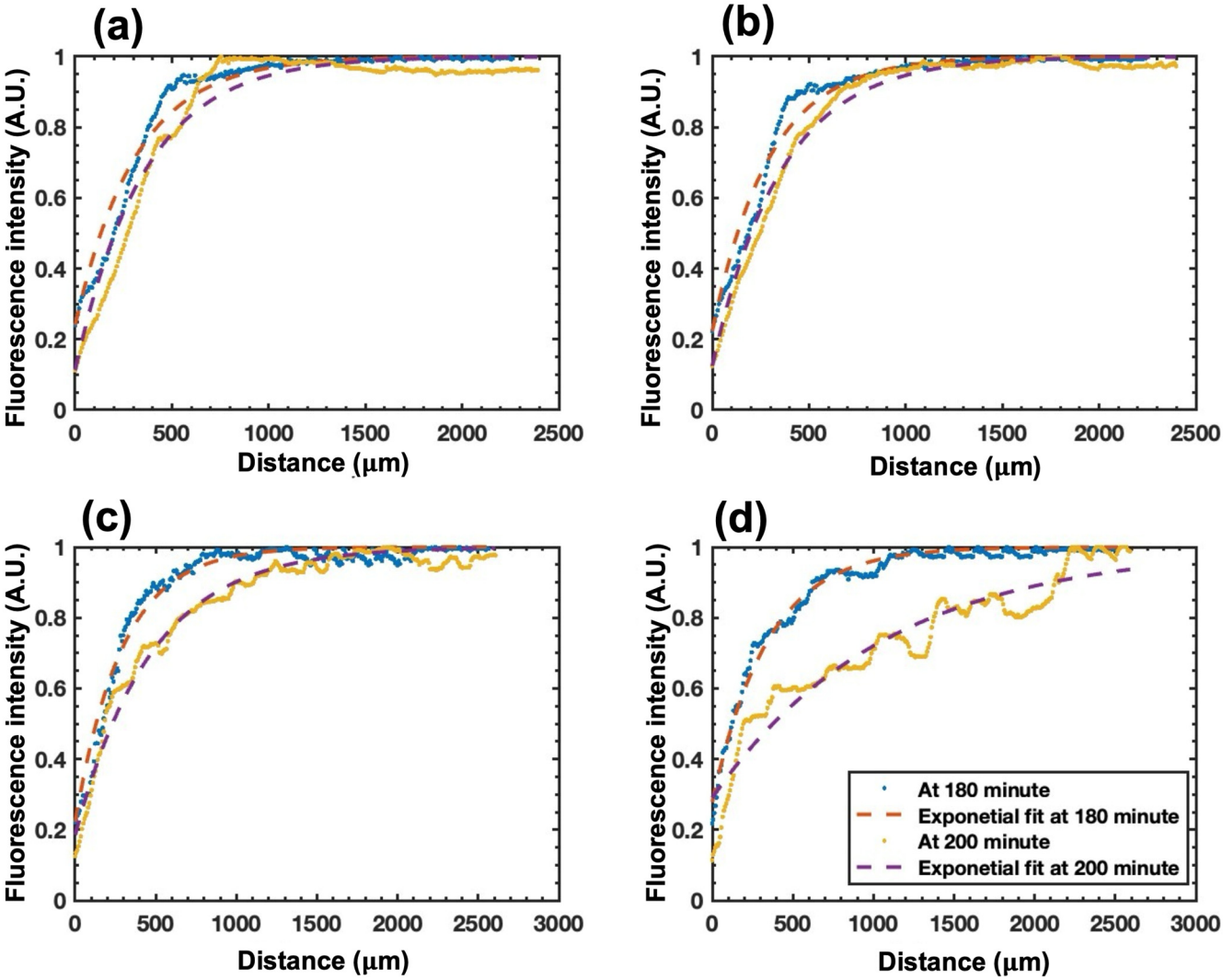

Figure 5. Fluorescent intensity profiles for pure oil and SDS-mixed oil at 180 and 360 min, along with their exponential fits. (**a**) Pure oil at 5 psig CO_2 pressure. (**b**) 2% (w/v) SDS mixed oil at 5 psig CO_2 pressure. (**c**) Pure oil at 10 psig CO_2 pressure. (**d**) 2% (w/v) SDS mixed oil at 10 psig CO_2 pressure.

To perform a comparative evaluation of the CO_2 diffusion rates in oil under different conditions, we estimate the distance corresponding to the identical change in normalized fluorescence intensity for different conditions of injection pressure and reduced surface tension of oil upon SDS addition. Table 1 summarizes the distances corresponding to changes in normalized fluorescence intensity (FI) from 0.2 to 0.9 under different conditions. It should be noted that a shorter distance for the same intensity change demonstrates a faster CO_2 diffusion rate in oil. The data show that adding SDS results in shorter distances for the same intensity change, indicating faster CO_2 diffusion in oil. For instance, the distance for the intensity changes from 0.2 to 0.9 is 895 μm in SDS–mixed oil at 10 psig and 360 min, compared to 2225.6 μm in pure oil. This pattern holds reasonably well in all conditions, with SDS–enhanced oil consistently showing shorter distances, thus demonstrating more efficient CO_2 diffusion over time. However, at 5 psig and 180 min, the distance for the intensity change from 0.2 to 0.9 in SDS–mixed oil (2320.7 μm) is unexpectedly higher compared to 5 psig without SDS (2358.2 μm). This anomaly is attributed to the less accurate fit of the pure oil data at 5 psig, and the difference is within the error range of multiple tests. Additionally, the change in CO_2 diffusion upon SDS addition at 5 psig is not as significant as observed at 10 psig. The overall trend, however, still supports the conclusion that adding SDS at higher injection pressure enhances the rate of CO_2 diffusion into the oil.

Table 1. Distances between two datapoints corresponding to fluorescence intensity (FI) change from 0.2 to 0.9 on the exponential fit for pure oil and SDS–mixed oil at 5 and 10 psig CO_2 pressures, measured at 180 and 360 min.

Injection Pressure		Distance [μm] (FI: 0.2 to 0.9)
5 psig CO_2	Pure oil at 180 min	2358.2
	Pure oil at 360 min	2395
	SDS-oil at 180 min	2399.9
	SDS-oil at 360 min	2320.7
10 psig CO_2	Pure oil at 180 min	2220.9
	Pure oil at 360 min	2225.6
	SDS-oil at 180 min	2008.1
	SDS-oil at 360 min	895.31

The increase in the rate of SDS-induced CO_2 dissolution into oil is largely attributed to the amphiphilic property of SDS. An amphiphilic molecule such as SDS has both a hydrophobic tail and a hydrophilic head, allowing it to interact with both oil and CO_2 [30]. Upon SDS addition into the system containing oil and CO_2, it reduces the surface tension between them, which makes CO_2 dissolution easier in oil. By adsorbing at the CO_2–oil interface, the SDS molecules lower interfacial tension (IFT), reducing the energy barrier for CO_2 transport across the interface (Figure 6). This lowered IFT enhances the mass transfer efficiency of CO_2 into the oil phase, enabling finer dispersion of CO_2 and increasing the contact area. Consequently, CO_2 molecules penetrate more effectively into the oil phase, improving their solubility and facilitating oil swelling.

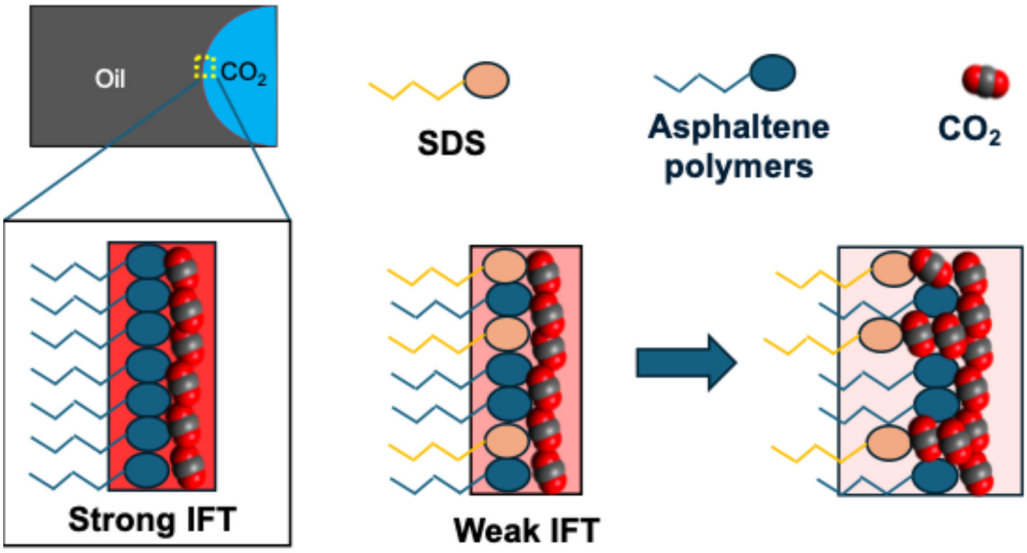

Figure 6. Illustrative image representing the reduced IFT between oil and CO_2 in presence of SDS.

In SDS, molecules naturally form structures called micelles, where the hydrophobic tails cluster together in the center, away from water, while the hydrophilic heads face outward, micelle formation is unlikely in oil at the low SDS concentrations used in our study [32]. Instead, SDS molecules aggregate at the CO_2-oil interface, creating localized microenvironments that enhance CO_2 absorption and solubility. This adsorption-driven mechanism modifies the diffusion pathways of CO_2, ensuring deeper penetration and uniform distribution into the oil phase. As a result, the enhanced dissolution of CO_2 leads to significant oil swelling, reducing the viscosity of the oil and improving its mobility.

3.2. Hybrid Huff-n-Puff in Micromodels

To evaluate the potential application of the proposed hybrid huff-n-puff in EOR, the micro reservoir model resembling the complex pore structure of the geologic reservoir was used for the flooding experiments. Initially, the micro reservoir model was vacuumed and filled with crude oil. The total amount of oil in the reservoir is known as the original oil-in-place (OOIP). As mentioned earlier, these flooding experiments were conducted in three stages: first flooding, oil swelling, and second flooding. For the flooding experiments, DI water and DI water with 2% (w/v) SDS surfactant were used as the flooding fluids to analyze the effect of SDS. In the first stage, flooding was performed with DI water or DI water–SDS at the flow rate of 20 μL/min for 30 min. This duration was selected based on the observation that flooding beyond 30 min yielded negligible additional oil recovery. The oil recovery was quantified through image processing of recorded video footage using MATLAB R2022b software. The process involved capturing an initial reference image of the oil-saturated porous medium before flooding to define OOIP. During the flooding process, changes in greyscale pixel values between the reference image and subsequent frames were analyzed to identify oil displacement, where darker regions represented oil and lighter regions indicated cleared areas. The pixel intensity differences were correlated to oil volume, providing a quantitative estimate of oil recovery. To ensure accuracy, consistent lighting conditions, camera calibration, and preliminary tests with known oil volumes were performed. This method has been used in many published articles [23]. Figure 7 shows time-dependent oil recovery during the first-stage flooding with pure DI water and SDS–DI water. In the case of pure DI water flooding, around 10% of OOIP was displaced over 30 min. Upon 2% (w/v) SDS addition in DI water, 13.5% oil recovery was achieved during the same flooding experiment period. This 3.5% improvement in oil recovery can be attributed to the adsorption mechanism of SDS surfactants, as explained earlier.

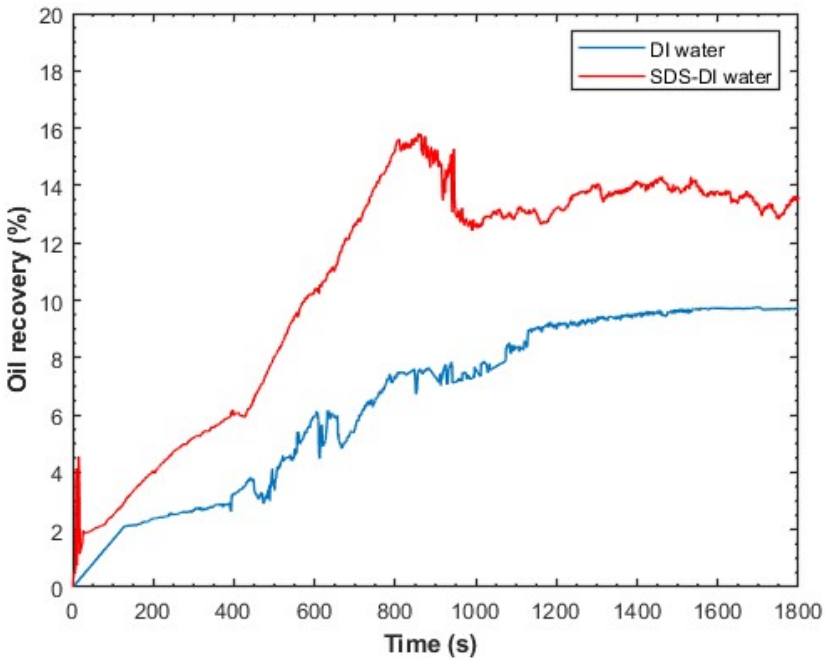

Figure 7. Oil recovery during DI water flooding and SDS–DI water flooding.

Upon analyzing the video to validate results, we found that the breakthrough during flooding occurred at 808 s and 850 s in DI water and SDS-DI water flooding, respectively. Although the 42 s delay is not significant, it can be attributed to the comparatively broader sweep volume of the pore network by SDS–DI water. In other words, the SDS–DI water solution could penetrate deeper into the pores and take longer to reach the production port than DI water. (The drop in oil recovery for SDS–DI water, as shown in Figure 7, is due

to a small disturbance observed around 850 s. After breakthrough, residual oil from the tiny pores was mobilized and carried into the main channels along with the flooding fluid. This caused a temporary drop in the recorded intensity values, which is reflected as a spike error in the recovery curve.) Due to the adsorption mechanism and IFT reduction caused by surfactants, the SDS–DI water solution was able to imbibe the oil from tiny pores more effectively, thereby sweeping a larger pore volume. The oil imbibition phenomena can be visually seen during the experiment, as shown in Figure 8 (see Supplementary Video S1). Two images were taken approximately at 30 min (almost at the end of the flooding) of the DI water and SDS–DI water flooding experiment. The highlighted section shows the exact pore network in both cases, where it is apparent in the red-circled area that SDS-DI water flooding could reach deeper into the pore network than DI water.

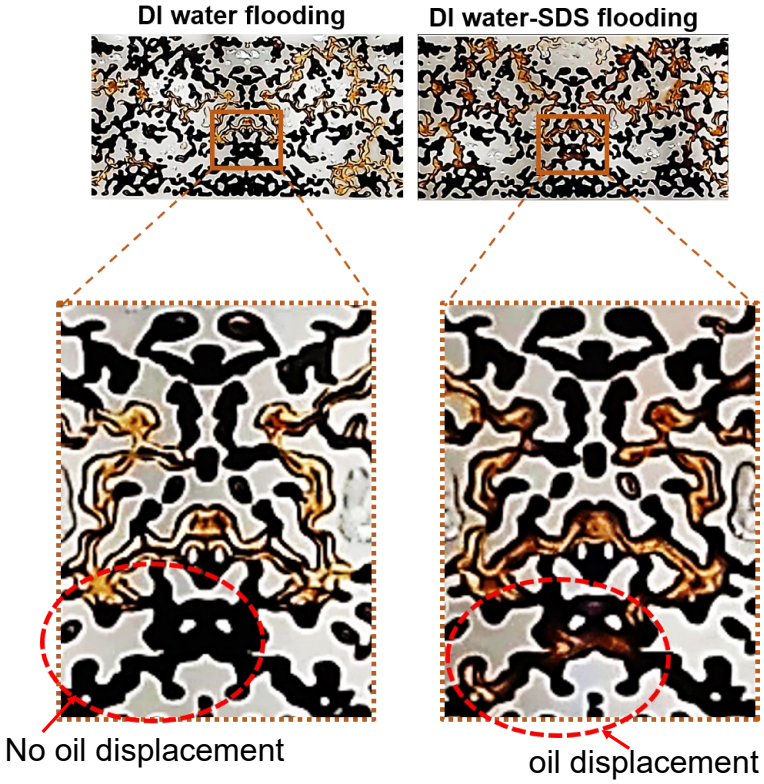

Figure 8. Comparison of oil displacement from the pore network between DI water and SDS–DI water flooding. The red circle shows the same area of the pore network in both cases where DI water flooding shows no oil displacement, whereas in DI water–SDS flooding, the oil shows being imbibed by flooding fluid. The image contrast has been changed for the visualization purpose.

To simulate the hybrid huff-n-puff process in the tested micromodel, after the first flooding stage, an intermediate oil swelling by CO_2 (i.e., soaking) for 6 h was performed, followed by second flooding. This 6 h duration was chosen based on previous fluorescence-based microscopic experiments for CO_2 dissolution in oil. In conventional CO_2-based oil swelling methods, such as huff-n-puff, oil recovery is primarily driven by the volume increase and reduced viscosity due to the swelling of the oil. However, the proposed hybrid approach can potentially enhance oil recovery further by incorporating this second flooding stage after the intermediate oil swelling stage. Chronologically, the first flooding stage recovers some oil but leaves a significant portion trapped in tiny pores. Subsequently, CO_2 is injected into the reservoir, causing the oil to swell and become more mobile, which adds to total oil recovery. After this intermediate swelling stage, the second flooding stage targets the remaining oil that was previously inaccessible. The removal of the swollen oil creates new pathways for trapped oil into tiny pores and reduces oil saturation, allowing the second flooding to sweep out additional oil that was previously trapped. This sequential

process maximizes oil recovery by combining the benefits of multiple operations. We would like to clarify that due to the low pressure of CO_2 and low SDS concentration, CO_2 foam was not observed.

We conducted a total of six different experiments, namely, DI water floodings with intermediate oil swelling and SDS–DI water floodings with intermediate oil swelling. Each case was repeated with three different CO_2 pressures of 5, 10, and 15 psig. The recorded experiments lasted 25,200 s, consisting of two 1800 s (30 min) of floodings and 21,600 s (6 h) of oil swelling. Figure 9a shows DI water flooding and oil swelling at 5 psig CO_2 pressure and second DI water flooding with their cumulative oil recovery in three different colors. The blue line shows the first flooding, which was 30 min long, and the line shows a steeper curve due to initial oil displacement. Following that, the orange-colored line shows CO_2-based oil swelling for 6 h. During this time, oil is not being recovered due to its swelling, the intensity value changes, and that change can be attributed to the slope of this line. Lastly, the yellow-colored line shows the second flooding, where the swelled oil is displaced. Due to the different time scales between flooding and oil swelling, it could be challenging to analyze the plot. Therefore, modifications were made to represent the complete plot of an experiment. In Figure 9b, the time axis has been trimmed from 5000 to 20,000 s to make the cumulative oil recovery visible in the plot for six different tests (Figure 10); for complete data, see Supplementary Information (SI).

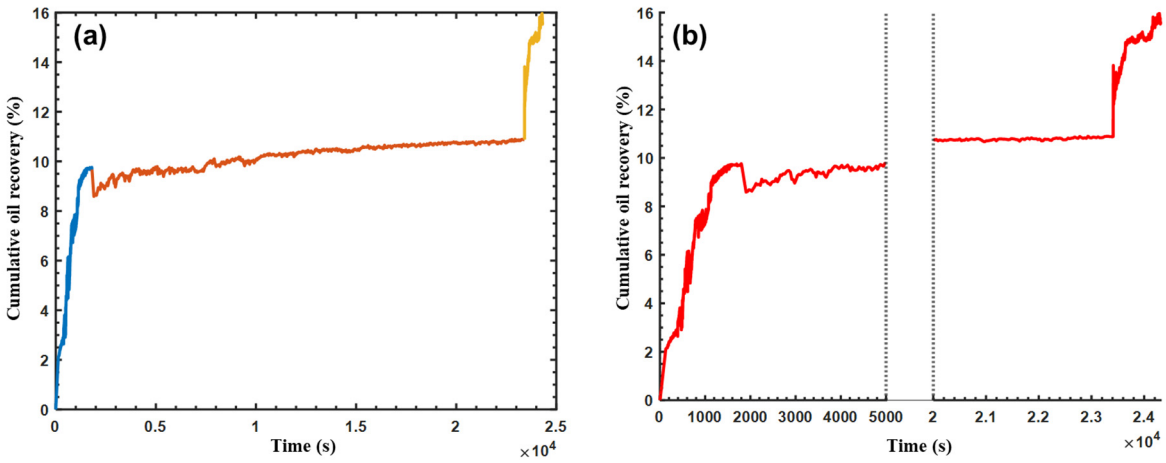

Figure 9. (**a**) Cumulative oil recovery during the DI water flooding with the intermediate oil swelling at 5 psig. First flooding (blue line), CO_2-based oil swelling (orange line), second flooding (yellow line). (**b**) Trimmed time axis for better representation of the plot.

Figure 10a,b show the cumulative oil recovery by DI water and SDS–DI water flooding at 5 psig CO_2 pressured oil swelling. DI water flooding-based CO_2 oil swelling produced around 16% of OOIP, whereas SDS-DI water flooding-based CO_2 oil swelling showed around 25% of oil recovery. This suggests that adding nonionic surfactant has been proven to improve oil recovery by 9%. Similarly, Figure 10c,d show the DI and SDS-DI water flooding at 10 psig pressured CO_2 oil swelling. The cumulative oil recovery in the DI water flooding case increased from 16% to 20%, whereas in the SDS–DI water flooding case, the cumulative oil recovery increased from 25% to 36% of OOIP. The improved oil recovery at 10 psig suggests that oil swelling is improved along with the higher pressure. However, the oil swelling at higher pressure yielded an increase of only 4% in the DI water case, whereas it was 10% for the SDS–DI water case, which shows a positive effect of SDS in oil swelling. Lastly, cumulative oil recovery at 15 psig CO_2 oil swelling is shown in Figure 10e,f. The DI water flooding case showed around 28% oil recovery. Even though 15 psig CO_2 pressured oil swelling with SDS–DI water flooding shows the highest oil recovery of approximately 37%, its improvement is very small compared to the previous 10 psig CO_2 pressured oil

swelling. Based on our data, we believe that oil production is almost at saturation at 10 psig with SDS–DI water.

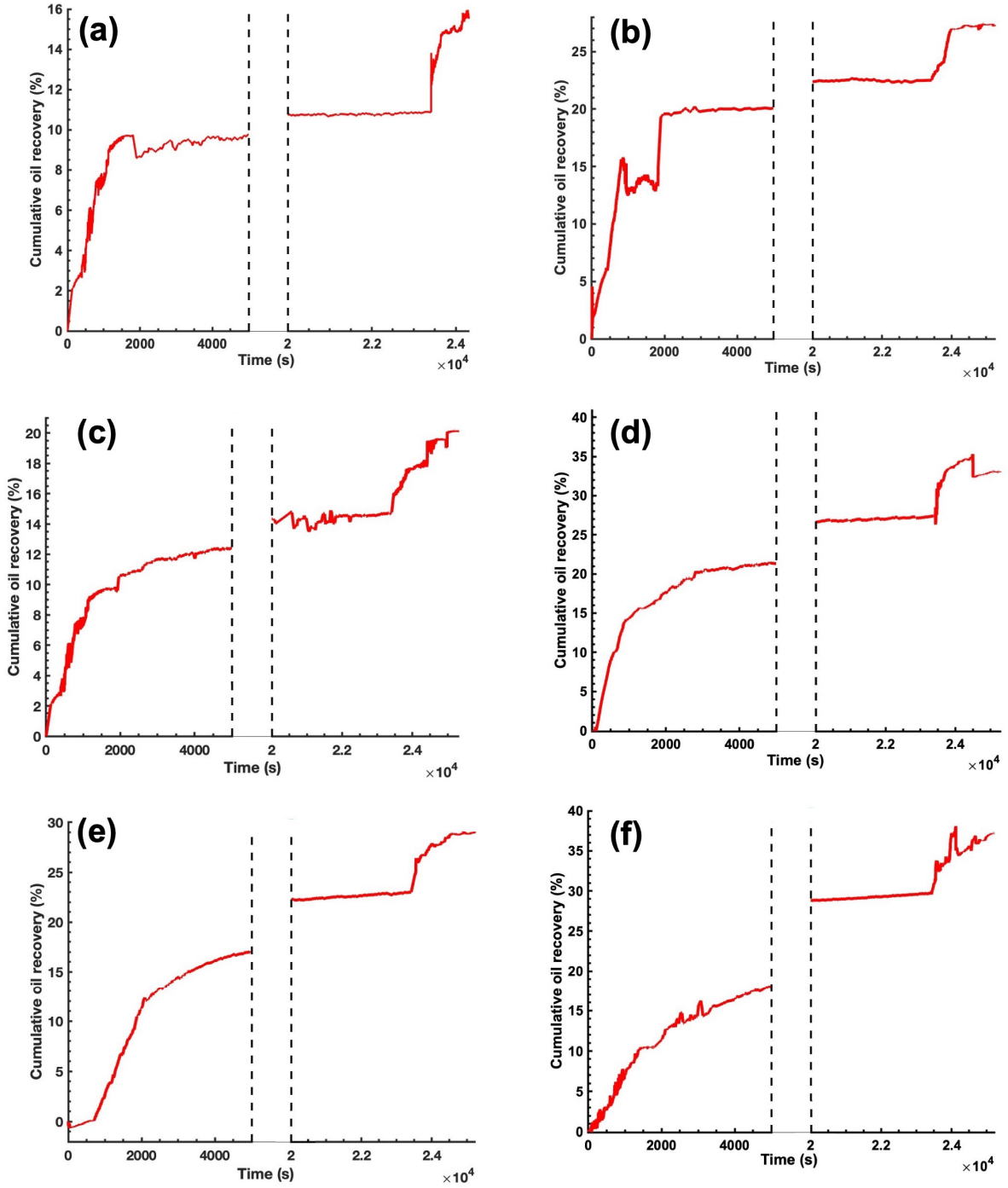

Figure 10. Cumulative oil recovery in flooding experiments. (**a**) DI water floodings with intermediate oil swelling at 5 psig. (**b**) SDS–DI water floodings with intermediate oil swelling at 5 psig. (**c**) DI water floodings with intermediate oil swelling at 10 psig. (**d**) SDS–DI water floodings with intermediate oil swelling at 10 psig. (**e**) DI water floodings with intermediate oil swelling at 15 psig. (**f**) SDS–DI water floodings with intermediate oil swelling at 15 psig.

4. Conclusions

This study represents an evaluation of the hydride huff-n-puff-based enhanced oil recovery (EOR) technique. The single-channel microfluidic experiments showed improved CO_2 dissolution in oil at low pressure upon the addition of 2% (w/v) SDS, attributing to

surfactant micelles formation at the CO_2–oil interface. The viability of the SDS-CO_2-assisted EOR via oil swelling was demonstrated by the huff-n-puff flooding using the 'reservoir-on-a-chip' approach with the PMMA-based micro reservoir. Six different experiments, including both DI water and SDS–DI water flooding with 5, 10 and 15 psig CO_2 pressured intermediate oil swelling, were tested. The DI water flooding showed a breakthrough at 808 s, whereas SDS–DI water flooding at 850 s. The 42 s delayed breakthrough can be attributed to the larger sweep area of SDS–DI water flooding compared to DI water flooding. The longer breakthrough time in SDS–DI water flooding is due to reduced interfacial tension and wettability alteration from the adsorption mechanism. The DI water-based flooding with 5 psig CO_2-pressured oil swelling showed cumulative oil recovery of 16% of OOIP. In the same experiment, the cumulative oil recovery was 25% with SDS–DI water flooding. At 10-psig CO_2 pressure, the cumulative oil recovery in DI water and SDS–DI water flooding was 20% and 36%, respectively. At 15-psig CO_2 pressure, the oil recovery was 28% and 37% in DI water and SDS-DI water flooding, respectively. The trend of achieving high oil recovery with higher pressure was maintained in the DI water flooding. However, in the case of SDS-DI water flooding, the improvement in oil recovery from 10 psig to 15 psig was less pronounced, possibly due to the saturation limit of oil recovery. This study concludes that the nonionic surfactant flooding with a CO_2-based intermediate oil swelling approach holds great promise as a future EOR method. To further validate the applicability of this method in reservoir recovery, future studies could focus on incorporating sandstone or carbonate rock-mimicking surfaces in the microchannel setup to better replicate geological reservoir conditions. Additionally, conducting core flooding experiments on actual reservoir cores or rock analogs would provide further insights into the performance of the method under more realistic reservoir conditions.

These advancements would help bridge the gap between laboratory-scale microfluidic studies and large-scale field applications, offering a clearer understanding of how different geological settings, such as sandstone and carbonate reservoirs, influencing the recovery mechanism.

Supplementary Materials: The following supporting information can be downloaded at: https://www.mdpi.com/article/10.3390/app142412078/s1, Figure S1: Comprehensive figure of cumulative oil recovery; Video S1: Flooding comparison with and without SDS

Author Contributions: Conceptualization, A.R. and M.K.; Methodology, A.R., J.D., M.P. and M.K.; Software, A.R.; Validation, A.R. and M.K.; Formal analysis, A.R., I.A. and M.K.; Investigation, A.R., J.D., M.P., I.A. and M.K.; Resources, M.K.; Data curation, A.R., J.D., C.S. and M.K.; Writing—original draft, A.R. and M.K.; Writing—review & editing, A.R., J.D., C.S., M.P., P.M., R.I.A.-R., R.I. and M.K.; Supervision, P.M., R.I.A.-R., R.I. and M.K.; Project administration, M.K. All authors have read and agreed to the published version of the manuscript.

Funding: This research was funded by the National Science Foundation, USA (grant number: 2207642).

Informed Consent Statement: Not applicable.

Data Availability Statement: The original contributions presented in the study are included in the article/Supplementary Material, further inquiries can be directed to the corresponding author.

Conflicts of Interest: The authors declare no conflict of interest.

References

1. BP, p.l.c. BP Energy Outlook 2019 Edition: The Energy Outlook. Available online: https://www.bp.com/en/global/corporate/news-and-insights/press-releases/bp-energy-outlook-2019.html (accessed on 18 December 2024).
2. International Energy Agency. *Key World Energy Statistics 2021*; International Energy Agency: Paris, France, 2021.
3. Miller, R.G.; Sorrell, S.R. The Future of Oil Supply. *Philos. Trans. R. Soc. A Math. Phys. Eng. Sci.* **2014**, *372*, 20130179. [CrossRef] [PubMed]
4. Alagorni, A.H.; Bin Yaacob, Z.; Nour, A.H. An Overview of Oil Production Stages: Enhanced Oil Recovery Techniques and Nitrogen Injection. *Int. J. Environ. Sci. Dev.* **2015**, *6*, 693. [CrossRef]

5. Godec, M.; Kuuskraa, V.; Van Leeuwen, T.; Melzer, L.S.; Wildgust, N. CO_2 Storage in Depleted Oil Fields: The Worldwide Potential for Carbon Dioxide Enhanced Oil Recovery. *Energy Procedia* **2011**, *4*, 2162–2169. [CrossRef]
6. Hu, B.; Gu, Z.; Zhou, C.; Wang, L.; Huang, C.; Su, J. Investigation of the Effect of Capillary Barrier on Water–Oil Movement in Water Flooding. *Appl. Sci.* **2022**, *12*, 6285. [CrossRef]
7. Alvarado, V.; Manrique, E. Enhanced Oil Recovery: An Update Review. *Energies* **2010**, *3*, 1529–1575. [CrossRef]
8. Mokheimer, E.M.A.; Hamdy, M.; Abubakar, Z.; Shakeel, M.R.; Habib, M.A.; Mahmoud, M. A Comprehensive Review of Thermal Enhanced Oil Recovery: Techniques Evaluation. *ASME. J. Energy Resour. Technol.* **2018**, *141*, 030801. [CrossRef]
9. Zallaghi, M.; Website, J.; Tajmiri, M.; Roozbehani, B. A Comprehensive Review of Chemical Induced Reservoir Wettability Alteration: Characterization and EOR Aspects American Journal of Oil and Chemical Technologies A Comprehensive Review of Chemical Induced Reservoir Wettability Alteration: Characterization and EOR Aspects. *Am. J. Oil Chem. Technol.* **2018**, *6*, 151–171.
10. Deng, X.; Tariq, Z.; Murtaza, M.; Patil, S.; Mahmoud, M.; Kamal, M.S. Relative Contribution of Wettability Alteration and Interfacial Tension Reduction in EOR: A Critical Review. *J. Mol. Liq.* **2021**, *325*, 115175. [CrossRef]
11. Sun, X.; Zhang, Y.; Chen, G.; Gai, Z. Application of Nanoparticles in Enhanced Oil Recovery: A Critical Review of Recent Progress. *Energies* **2017**, *10*, 345. [CrossRef]
12. Zhou, X.; Yuan, Q.; Peng, X.; Zeng, F.; Zhang, L. A Critical Review of the CO_2 Huff 'n' Puff Process for Enhanced Heavy Oil Recovery. *Fuel* **2018**, *215*, 813–824. [CrossRef]
13. Nguyen, T.-L.; Hoang, A.-Q.; Pham, D.-K.; Hamza, M.F.; Sinnathambi, C.M.; Merican, M.A. Recent Advancement of Hybrid Materials Used in Chemical Enhanced Oil Recovery (CEOR): A Review. *IOP Conf. Ser. Mater. Sci. Eng.* **2017**, *206*, 012007. [CrossRef]
14. Rego, F.B.; Botechia, V.E.; Schiozer, D.J. Heavy oil recovery by polymer flooding and hot water injection using numerical simulation. *J. Pet. Sci. Eng.* **2017**, *153*, 187–196. [CrossRef]
15. Li, Q.; Li, Q.; Wang, F.; Wu, J.; Wang, Y. The Carrying Behavior of Water-Based Fracturing Fluid in Shale Reservoir Fractures and Molecular Dynamics of Sand-Carrying Mechanism. *Processes* **2024**, *12*, 2051. [CrossRef]
16. Li, Q.; Li, Q.; Han, Y.A. Numerical Investigation on Kick Control with the Displacement Kill Method during a Well Test in a Deep-Water Gas Reservoir: A Case Study. *Processes* **2024**, *12*, 2090. [CrossRef]
17. Sayegh, S.G.; Maini, B.B. Laboratory Evaluation of the CO_2 Huff-N-Puff Process for Heavy Oil Reservoirs. *J. Can. Pet. Technol.* **1984**, *23*, 29–36. [CrossRef]
18. Simpson, M.R. The CO_2 huff'n'puff process in a bottomwater-drive reservoir. *J. Pet. Technol.* **1988**, *40*, 887–893. [CrossRef]
19. Murray, M.D.; Frailey, S.M.; Lawal, A.S. New approach to CO_2 flood: Soak alternating gas. In Proceedings of the SPE Permian Basin Oil and Gas Recovery Conference, Midland, TX, USA, 15–17 May 2001; SPE: Kuala Lumpur, Malaysia, 2001; p. SPE-70023.
20. Lv, W.; Gong, H.; Dong, M.; Li, Y.; Sun, H.; Sun, Z.; Jiang, H. Potential of Nonionic Polyether Surfactant-Assisted CO_2 Huff-n-Puff for Enhanced Oil Recovery and CO_2 Storage in Ultra-Low Permeability Unconventional Reservoirs. *Fuel* **2024**, *359*, 130474. [CrossRef]
21. Kalam, S.; Abu-Khamsin, S.A.; Kamal, M.S.; Patil, S. A Review on Surfactant Retention on Rocks: Mechanisms, Measurements, and Influencing Factors. *Fuel* **2021**, *293*, 120459. [CrossRef]
22. Kumar Gunda, N.S.; Bera, B.; Karadimitriou, N.K.; Mitra, S.K.; Hassanizadeh, S.M. Reservoir-on-a-Chip (ROC): A New Paradigm in Reservoir Engineering. *Lab Chip* **2011**, *11*, 3785–3792. [CrossRef] [PubMed]
23. Hafez, M.; Ratanpara, A.P.; Martiniere, Y.; Dagois, M.; Ghazvini, M.; Kavosi, M.; Mandin, P.; Kim, M. CO_2-Monoethanolamine-Induced Oil Swelling and Viscosity Reduction for Enhanced Oil Recovery. *J. Pet. Sci. Eng.* **2021**, *206*, 109022. [CrossRef]
24. Ratanpara, A.; Kim, M. Wettability Alteration Mechanisms in Enhanced Oil Recovery with Surfactants and Nanofluids: A Review with Microfluidic Applications. *Energies* **2023**, *16*, 8003. [CrossRef]
25. Seo, S.; Mastiani, M.; Mosavati, B.; Peters, D.M.; Mandin, P.; Kim, M. Performance evaluation of environmentally benign nonionic biosurfactant for enhanced oil recovery. *Fuel* **2018**, *234*, 48–55. [CrossRef]
26. Nayak, N.; Yue, C.; Lam, Y.; Tan, Y. Thermal Bonding of PMMA: Effect of Polymer Molecular Weight. *Microsyst. Technol.* **2010**, *16*, 487–491. [CrossRef]
27. Genuino, H.C.; Horvath, D.T.; King'Ondu, C.K.; Hoag, G.E.; Collins, J.B.; Suib, S.L. Effects of Visible and UV Light on the Characteristics and Properties of Crude Oil-in-Water (O/W) Emulsions. *Photochem. Photobiol. Sci.* **2012**, *11*, 692–702. [CrossRef]
28. Gong, B.; Zhang, H.; Wang, X.; Lian, K.; Li, X.; Chen, B.; Wang, H.; Niu, X. Ultraviolet-Induced Fluorescence of Oil Spill Recognition Using a Semi-Supervised Algorithm Based on Thickness and Mixing Proportion–Emission Matrices. *Anal. Methods* **2023**, *15*, 1649–1660. [CrossRef] [PubMed]
29. Li, H.; Zheng, S.; Yang, D. Enhanced Swelling Effect and Viscosity Reduction of Solvent(s)/CO_2/Heavy-Oil Systems. *SPE J.* **2013**, *18*, 695–707. [CrossRef]
30. Li, L.; Zheng, J.; Shi, Y.; Su, Y.; Hao, Y.; Chen, Z. Mechanisms of Fluid Migration and CO_2 Storage in Low Permeability Heavy Oil Reservoirs Using High-Pressure Microfluidic CO_2 Flooding Experiment. *Energy Fuels* **2024**, *38*, 7997–8008. [CrossRef]

31. Sharbatian, A.; Abedini, A.; Qi, Z.; Sinton, D. Full Characterization of CO_2-Oil Properties On-Chip: Solubility, Diffusivity, Extraction Pressure, Miscibility, and Contact Angle. *Anal. Chem.* **2018**, *90*, 2461–2467. [CrossRef] [PubMed]
32. Hammouda, B. Temperature Effect on the Nanostructure of SDS Micelles in Water. *J. Res. Natl. Inst. Stand. Technol.* **2013**, *118*, 151. [CrossRef] [PubMed]